Engineering Geology 277 (2020) 105786

Contents lists available at ScienceDirect

Engineering Geology

journal homepage: www.elsevier.com/locate/enggeo

New developments for the performance-based assessment of seismically-induced slope displacements

Jorge Macedo[a,*], Gabriel Candia[b], Maxime Lacour[c], Chenying Liu[a]

[a] Georgia Institute of Technology, Atlanta, GA, United States of America
[b] Facultad de Ingeniería Civil, Universidad del Desarrollo, Chile, and National Research Center for Integrated Natural Disaster Management ANID/FONDAP/15110017, Santiago, Chile
[c] Univ. of California, Berkeley, CA, United States of America

A B S T R A C T

This study presents new developments for the performance-based assessment of seismically-induced slope displacements (D). Performance-based procedures enable a hazard-consistent and rational seismic design of slope systems; hence, their use in practice is appealing. However, they are not the standard in engineering practice because their use is considered too complex to be used for non-critical projects. The developments presented in this study allow the straightforward estimation of displacement hazard curves (DHC) for a wide range of slope systems subjected to earthquakes in different tectonic settings (i.e., shallow crustal, and subduction), considering a rigorous quantification of the existing uncertainties.

The new developments include 1) full integration of probabilistic seismic hazard assessments (PSHA), and the estimation of DHCs, 2) automatic estimation of DHC for D models with multiple intensity measures through vector PSHA, 3) estimation of DHC for systems with contributions from multiple tectonic settings, 4) uncertainty treatment (i.e., epistemic and aleatory) on DHCs, through a logic tree scheme, 5) deaggregation of earthquake scenarios from DHCs, and 6) uncertainty quantification on DHCs through the polynomial chaos theory. The new developments are implemented in a MATLAB graphical user interface (GUI) to facilitate its use by engineers and researchers. We discuss illustrative examples and guidelines for the application of the GUI to evaluate the seismic performance of different slope systems that are affected by earthquakes from multiple tectonic settings.

1. Introduction

The evaluation of the seismic performance of slope systems (e.g., earth and waste slopes, natural slopes) in engineering practice often relies on estimating the amount of seismically induced displacements (D) through analytical procedures. The existing approaches to estimate D are summarized in Macedo et al. (2018), which are in general classified as 1) deterministic-based, 2) pseudo-probabilistic, and 3) performance-based probabilistic approach (PBPA). These approaches rely on analytical D models, usually defined in terms of slope properties and intensity measures (IMs) that represent the seismic demand for the estimation of D. In a deterministic-based approach, the first step consists of using a single ground motion model (GMM), an earthquake scenario (i.e., magnitude, distance), and site conditions to estimate the IM of interest. The estimated IM is then used as an input in a D model. The deterministic approach can incorporate uncertainties in the D or/and IMs estimates by adding standard deviations above or below median values.

At present, the pseudo-probabilistic approach is the procedure most used in practice. The first step consists of a probabilistic seismic hazard assessment (PSHA) to estimate an IM hazard curve (usually the mean IM hazard), which provides the mean annual rate of exceedance for different IM values. Then, the engineer defines a hazard level or return period, which often relies on regulatory guidance, and selects the corresponding IM value from the estimated IM hazard curve. Finally, the selected IM value is used as an input in a D model, which provides a D estimate. The standard deviation of the D model could also be considered to include some uncertainty in the D estimate. This approach has the implicit assumption that the hazard design level for IM is consistent with that of D. However, this assumption does not have a rational basis and may not be appropriate (Macedo, 2017; Rathje and Saygili, 2011).

In a PBPA, an IM hazard curve is also obtained from a PSHA, but in this case, the IM hazard is combined with a D model through a convolution process. Importantly the convolution considers all the variability in the adopted D model. The outcome is a D hazard curve (DHC), which provides the mean annual rate of exceedance for different D values. Several percentiles of the IM hazard curve may be used, but a common practice is to use only the mean IM hazard curve, as it is often considered that the IM uncertainties have been accounted for in the PSHA (Wang and Rathje, 2015). Importantly, a proper PBPA-based evaluation should consider the full range of epistemic uncertainty

* Corresponding author.
E-mail addresses: jorge.macedo@gatech.edu (J. Macedo), gcandia@udd.cl (G. Candia), maxlacour@berkeley.edu (M. Lacour), cliu662@gatech.edu (C. Liu).

https://doi.org/10.1016/j.enggeo.2020.105786
Received 23 December 2019; Received in revised form 24 July 2020; Accepted 27 July 2020
Available online 31 July 2020

associated with alternative D models in the estimation of DHCs. A more complete PBPA, herein referred to as a Fully Probabilistic Performance-Based Approach (FPPBA), considers the full set of IM percentiles for the estimation of DHCs. The authors are not aware of published FPPBA applications accounting for realistic earthquake scenarios and seismic sources as those found in engineering projects.

PBPA or FPPBA approaches should be preferred in geotechnical earthquake engineering, because they better incorporate the uncertainties in the IM and the properties of a slope system, in addition, they provide a solid framework for hazard informed decisions.

Importantly, PBPA and FPPBA approaches provide D estimates that can be directly related to a prescribed hazard design level. This is because the hazard is quantified based on a relevant index of seismic performance, which is D, and not on an indirect index of performance such as an IM, as traditionally considered in pseudo probabilistic procedures. However, PBPA or FPPBA approaches are not commonly used in practice because its implementation is often considered cumbersome.

This study presents new developments for the estimation of D using the PBPA and FPPBA frameworks, which are implemented in MATLAB-based computational platform that enables the straightforward application of PBPA and FPPBA approaches in engineering practice. The procedures presented in this paper allow estimating DHCs for slopes located in different tectonic settings, considering a rigorous quantification of the existing uncertainties and realistic scenarios as those found in engineering projects. In addition, our implementations can be used to perform a direct comparison between the PBPA and FPPBA approaches. As discussed before, the few reported applications (i.e., Macedo et al., 2018; Wang and Rathje, 2015) have typically considered only a PBPA framework. Hence, it is not clear if using only the mean IM hazard curve can introduce substantial biases in DHC estimations.

2. Previous studies and implementations

PBPA or FPPBA based procedures rely on robust probabilistic models to estimate D. These models are typically formulated based on Newmark-based sliding block analyses and can be broadly categorized as:

(1) Models based on rigid-sliding blocks: These models do not account for the dynamic response of the sliding mass, and hence they do not consider the sliding mass flexibility (e.g., Newmark, 1965; Richards and Elms, 1979; Lin and Whitman, 1986; Watson-Lamprey and Abrahamson, 2006; Jibson, 2007; Saygili and Rathje, 2008).
(2) Decoupled D models: in these models the dynamic response of the sliding mass is computed independently from the seismically-induced displacements. In a first step, the dynamic response of the sliding mass is evaluated under the assumption of no relative displacements. Then, the system's dynamic response (e.g., acceleration time histories) is used to evaluate D (e.g., Makdisi and Seed, 1978, Bray and Rathje 1998, Rathje and Antonakos, 2011).
(3) Coupled D models: These models are based on analyses that account simultaneously for the dynamic response of the sliding mass and the generation of seismically-induced displacements. In the literature, these models are also known as fully coupled stick-slip models (e.g., Bray and Travasarou, 2007; Macedo et al., 2017; Du et al., 2018; Bray et al., 2018; Bray and Macedo, 2019).

The procedures to estimate D can also be grouped by their applicability to different tectonic settings. For instance, the Bray et al. (2018) method is currently the only robust procedure to estimate D in subduction zones (e.g., South America); this method has been formulated based on a large ground motion dataset and validated against well-documented case histories. On the other hand, there are several procedures available for shallow crustal tectonic settings (e.g., the West coast in the United States), including most of the procedures just discussed in the previous paragraphs. Finally, we are not aware of procedures strictly applicable to stable continental zones such as the central and eastern United States.

The computation of a DHC requires a D model and knowledge of the IM hazard. For instance, using the Bray and Macedo (2019) and Bray et al. (2018) D models, a DHC can be estimated from a single IM as (Macedo et al., 2018):

$$\lambda_D = \sum_{i=1}^{nky} \sum_{j=1}^{nTs} \int_0^\infty P\,(D > d \mid IM,\, k_{yi},\, T_{sj}) \Delta\lambda_{IM}\, d(IM) w_i w_j \tag{1}$$

where T_s is the sliding mass's initial fundamental period and k_y the yield coefficient. The term $P\,(D > d|IM,\, k_{yi},\, T_{sj})$ is the probability that D exceeds a threshold level d conditioned on IM, k_y and T_s, and $\Delta\lambda_{IM}$ represent the IM annual rate of occurrence. The uncertainties in the slope parameters k_y and T_s are treated as epistemic. Thus, a logic tree is employed, in which nky alternative values for k_y are defined with weighting factors w_i ($i = 1 : nky$) and nTs alternative values for T_s are defined with weighting factors w_j ($j = 1 : n$Ts). The alternative k_y and T_s values, and their corresponding weights in the logic tree may be obtained from a lognormal distributions as discussed in Macedo et al. (2018).

For cases where the D model is formulated in terms of two intensity measures, say $IM1$ and $IM2$, and without considering the epistemic uncertainty associated with alternative D models, a DHC can be estimated as:

$$\lambda_D = \sum_{i=1}^{nky} \sum_{j=1}^{nTs} \int_0^\infty \int_0^\infty P\,(D > d \mid IM1,\, IM2,\, k_{yi},\, T_{sj}) \Delta\lambda_{IM1,IM2}\, d(IM1) d(IM2) w_i w_j \tag{2}$$

where $\Delta\lambda_{IM1,\,IM2}$ is the joint annual rate of occurrence for $IM1$ and $IM2$ and is calculated from vector PSHA (see the "implementations" section); the remaining terms are analogous to Eq. (1).

Eqs. (1) and (2) assume that the IM hazard information from a PSHA study is available, which can be an important limitation. While scalar hazard information for some spectral accelerations is available from public online tools (e.g., the Unified Hazard Tool, USGS, 2017 in the U.S.), this is not necessarily the case for other regions (e.g., South America). Furthermore, in most cases, these tools provide no information regarding the different IM hazard percentiles or vector PSHA information required for FPPBA evaluations.

In terms of existing implementations to estimate DHCs, Macedo et al. (2018) provide scripts to estimate DHCs applicable to simplified seismic sources and the Bray and Travasarou (2007) and Bray et al. (2018) models separately. Saygili et al. (2018) provide Jupyter notebooks that implement the Rathje et al. (2014) models for the estimation of DHC. These implementations cannot be applied to cases where there is a contribution from multiple tectonic settings since they are developed for shallow crustal settings. In addition, these implementations are not fully automated because they require the user to input the IM hazard information (e.g., the Saygili et al., 2018 Jupyter notebooks require PGV estimates, and the Macedo et al., 2018 scripts require the hazard information for the spectral acceleration at the slope's degraded period). This is particularly inconvenient for D models formulated in terms of more than one IM, where vector hazard IM assessments are needed. Thus, for the straightforward evaluation of DHCs in practice, implementations that integrate the IM hazard and the estimation of the D hazard are necessary. Finally, the existing implementations do not incorporate the epistemic uncertainty from alternative D models, they do not allow FPPBA assessments, and they do not provide a rigorous and efficient quantification of uncertainties in D hazard curves. In this manuscript, we present new developments and implementations to address these gaps.

3. NEW developments for displacement hazard assessment

This section presents the new developments and implementations performed in this study for the PBPA and FPPBA assessment of slope

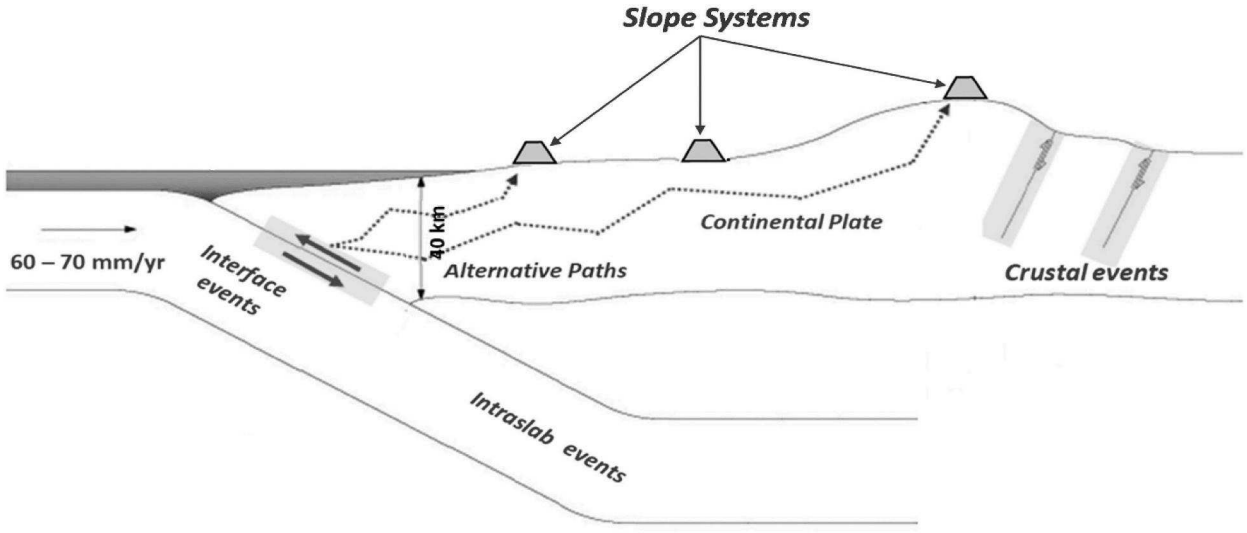

Fig. 1. General tectonic setting configuration considered in this study. Seismically-induced displacements in slope systems can be generated by earthquakes from shallow crustal and subduction (interface, intraslab) earthquake zones.

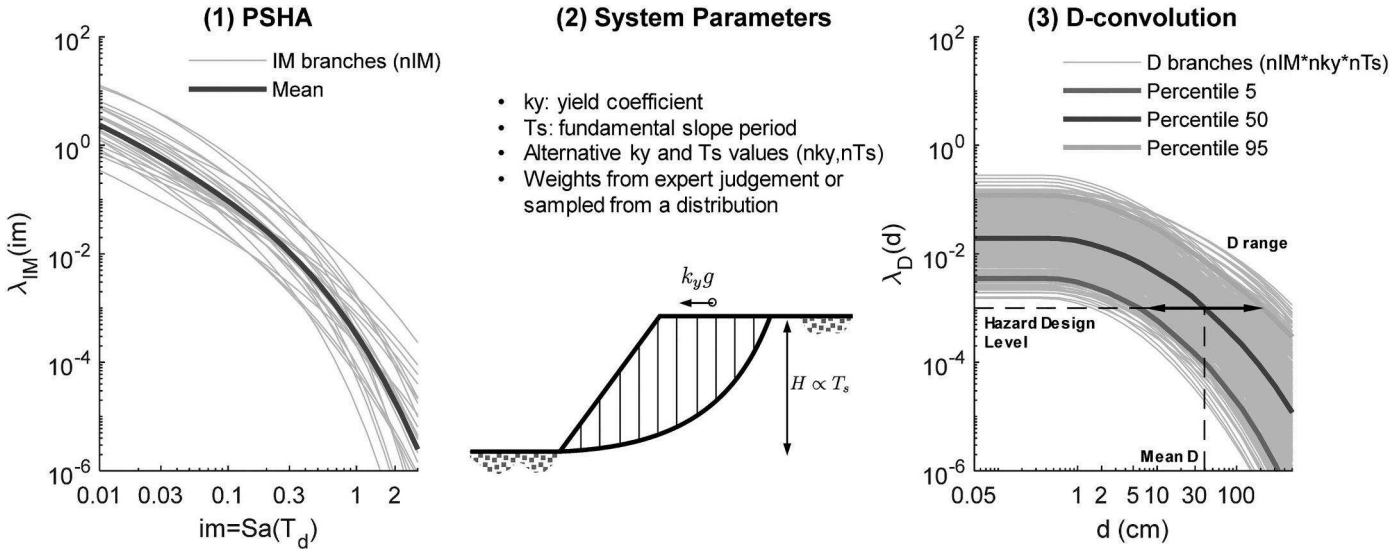

Fig. 2. Steps of the FPPBA procedure developed in this study, considering a single D model.

systems using D as the performance index. The new developments and implementations include fully integrated PSHA and displacement calculations (including scalar and vector hazard), estimation of DHCs for systems with contributions from multiple tectonic settings, deaggregation of earthquake scenarios from DHCs, uncertainty treatment through logic trees in PBPA and FPPBA approaches, and uncertainty treatment through the polynomial chaos (PC) theory. The new developments are implemented in a MATLAB graphical user interface (GUI) to facilitate its use in the geotechnical earthquake engineering community.

3.1. General framework

Fig. 1 shows the configuration of seismic sources and tectonic settings considered in this study. A slope system can be affected by earthquakes from shallow crustal tectonic settings, subduction tectonic settings (interface and intraslab), or a combination of them.

In this general setup, the scalar IM hazard is estimated according to:

$$\lambda_{IM}(IM > z) = \sum_{i=1}^{N_S} N^i(M_{min}) \int_{M_{min}}^{M^i_{max}} \int_0^{R_{max}} P(IM > z \mid m, r) f_M^i(m) f_R^i(r \mid m) dr dm \quad (3)$$

which is the well-known PSHA equation in its simplest form. Eq. (3) has the following key components: N_s is the total number of seismic sources considering shallow crustal and subduction mechanisms (interface, intraslab), the term $N^i(M_{min})$ is the activity rate of the i-th seismic source, defined as the average number of earthquakes per year with magnitude greater or equal to a magnitude threshold M_{min}, the term $P(IM > z|m, r)$ is the probability that IM exceeds z given an earthquake of magnitude m at a distance r from the source and is obtained from GMMs. Finally, the term $f_M^i(m)$ is the probability density function (PDF) for the earthquake magnitude distribution of the i-th source, and $f_R^i(r|m)$ is the PDF of the site-to-source distance, which is a function of the site location, the source geometry, and the adopted rupture area model.

3.2. Fully probabilistic performance-based approach

In a FPPBA the full set of IM percentiles are used to estimate a full set of DHCs (i.e., the mean DHC and D hazard percentiles); this process consists of three steps and is illustrated in Fig. 2 for a single D model (the case with multiple D models is discussed later). The first step is conducting a seismic hazard analysis for the IM of interest, evaluating

Eq. (3) for *nIM* realizations of the epistemic uncertainty (i.e., *nIM* branches in a logic tree structure) will result in *nIM* alternative hazard curves, with corresponding weighting factors w_k ($k = 1 \ldots nIM$). Then, generate samples *nky* and *nTs* of the slope parameters k_y and T_s, respectively, and assign weights to each realization (e.g., from a probability distribution). Finally, using a D-model each hazard curve is convolved with the D fragility function associated to each of the *nky* realizations for the yield coefficient and the *nTs* realizations of the initial fundamental period, resulting in $nIM \cdot nky \cdot nTs$ realizations for the DHCs. Analogous to the mean IM hazard curve computed from multiple GMMs and the use of weighting factors w_k, the mean DHC can be computed as the weighted average of alternative DHCs, each having a weighting factor $w_i \cdot w_j \cdot w_k$. In addition, as illustrated in Fig. 2, if a hazard design level is provided, then the D percentiles consistent with the hazard design level can be estimated from the set of DHCs (e.g., see the D range for the 5–95 percentiles).

3.3. Estimation of DHC considering multiple tectonic settings

Depending on the particular tectonic setting where a slope system is located, multiple seismic sources may contribute to the D hazard. For instance, slope systems on the South American coast could be affected by shallow crustal and subduction earthquakes, and a similar situation occurs in the Pacific Northwest of the United States.

For a seismic setting consisting of ${N_s}^{SC}$ shallow crustal sources, ${N_s}^{SI}$ subduction interface sources, and ${N_s}^{SS}$ subduction intraslab sources, Eq. (3) can be applied separately to each source type to obtain the IM hazard curves ${\lambda_I}^{SC}$, ${\lambda_I}^{SI}$, and ${\lambda_I}^{SS}$, which are the hazard contributions from shallow crustal, subduction interface, and subduction intraslab earthquakes, respectively. In addition, the annual rate of occurrence $\Delta\lambda_{IM}$ for each source group (SC or SI or SS) and representative of the *IM* bin interval $[IM_j \; IM_{j+1}]$, can be written in discrete form as:

$$\Delta\lambda_{IM} = -\frac{d\lambda_{IM}}{d(IM)} \approx -\frac{\lambda_{IM_j} - \lambda_{IM_{j+1}}}{IM_j - IM_{j+1}} = \frac{RO_{IM}}{IM_j - IM_{j+1}} \tag{4}$$

where $RO_{IM} = \lambda_{IMj} - \lambda_{IMj+1}$, is the rate of occurrence of the ground motion intensity IM_j.

The DHC, for each mechanism, can now be evaluated according to Eq. (1), using a D model consistent with the tectonic setting being considered i.e., a D model for shallow crustal sources should be convolved with the ${\lambda_{IM}}^{SC}$ hazard curve and a D model for interface settings with ${\lambda_D}^{SI}$ and so on. We will denote ${\lambda_D}^{SC}$, ${\lambda_D}^{SI}$, and ${\lambda_D}^{SS}$, as the D annual rate of exceedances for shallow crustal, subduction interface, and subduction intraslab earthquakes, respectively. In this manner, the contributions from different tectonic settings to the total D hazard can be evaluated. In cases where the D models are formulated in terms of two IMs, Eq. (2) is used instead in a similar fashion. These procedures are available in the developed GUI and are fully coupled with PSHA capabilities (see the implementations section for details).

3.4. Epistemic uncertainty treatment in D models through logic trees

In PBPA or FPPBA evaluations, uncertainties are typically categorized as 1) aleatory variability, which is associated with the natural randomness in a process, and 2) epistemic uncertainty, which is associated with the scientific uncertainty in the model of a process and is due to limited data and knowledge. In the former, the randomness is parametrized by probability values or probability density functions; in the later, the uncertainty is characterized by alternative models. In addition, there is epistemic uncertainty in parameters that are not random but have only a single correct (but unknown) value. In the particular case of slope systems, the epistemic uncertainty is often characterized by alternative D models and alternative realizations in the slope system properties. An adequate treatment of epistemic uncertainties is important because it affects the estimated D hazard percentiles. Eq. (1) (or more general forms of this equation) already accounts for the epistemic uncertainties associated with the slope system properties; however, the epistemic uncertainty for alternative D models also needs to be considered. Similar to the process illustrated in Fig. 2, additional branches are required to represent the alternative D models in the logic tree structure; each D model is assigned a weighting factor w_l, where $l = 1 : nD$, and *nD* is the number of alternative D models considered. Hence, a more robust logic tree may consider up to $nT = nIM \cdot nky \cdot nTs \cdot nD$ branches, in which the weighting factor of the branch that combines the *k*-th IM hazard curve, the *i*-th yield coefficient, the *j*-th fundamental period, and the *l*-th D model is simply $w_{i,j,k,l} = w_i \cdot w_j \cdot w_k \cdot w_l$. The logic tree branches are built separately for each tectonic setting (SC or SS or SC), resulting in *nT* realizations of ${\lambda_D}^{SC}$, ${\lambda_D}^{SI}$, and ${\lambda_D}^{SS}$. Finally, these realizations can be added to get the total mean annual rate of exceedance of slope displacements λ_D as:

$$\lambda_D = \sum_{i=1}^{nky} \sum_{j=1}^{nTs} \sum_{k=1}^{nIM} \sum_{l=1}^{nD} \{(\lambda_D^{SC} + \lambda_D^{SI} + \lambda_D^{SS})_{i,j,k,l} \cdot w_{i,j,k,l}\} \tag{5}$$

The full set of realizations can also be used to estimate the percentiles of D hazard curves. The process just described is consistent with the FPPBA framework. In the case of PBPA approach, the formulation uses an average IM hazard curve for each mechanism (SC or SI or SS) based on weights w_k of the alternative IM hazard curves.

3.5. Magnitude and distance deaggregation of displacement hazard

Let's consider a combination of *nMag* magnitudes, *nDist* site-to-source distance values, and *neps* epsilon values (where epsilon is the number of standard deviations above the median IM) in the implementation of Eq. (3), which results in a total number of ground motion scenarios $nScen = nMag \cdot nDist \cdot neps$. In addition, consider *nl* levels for *IM*, and *ndl* levels for D in Eq. (1). The IM hazard values from Eq. (3) can be stored in the matrix $[\lambda_{IMT}]_{nScen \times nl}$, where a row is associated with a scenario, and a column with an *IM* value. Based on Eq. (4), we define the *IM* annual rate of occurrence matrix as $[\Delta\lambda(IMT)]_{nScen \times nl}$; to ensure that $[\Delta\lambda(IMT)]$ and $[\lambda(IMT)]$ have the same dimensions, the *nl*-th column of the occurrence matrix is a duplicate of the $(nl - 1)$-th column.

Now, for a fixed D level, and fixed k_y and T_s values, we can evaluate Eq. (1) for each scenario and at each IM level considered; the result of this operation, denoted herein as $[PS\lambda_D]_{nScen \times nl}$, is a matrix that contains the partial annual rate of exceedances sorted by scenarios and IM values. Finally, the D hazard contribution from all IM levels is computed by adding the columns of $[PS\lambda_D]$, resulting in a column vector of length *nScen*, denoted hereafter $S\lambda_D = [S\lambda_{D1}, S\lambda_{D2}, \ldots, S\lambda_{DnScen}]^T$. This vector can be used as a proxy to perform the deaggregation of the DHC as follows:

$$Deagg_{Di} = S\lambda_{Di} / \sum_{p=1}^{nScen} S\lambda_{D,p} \tag{6}$$

In Eq. (6) $Deagg_{di}$ contains the deaggegration for an earthquake scenario. In this manner, a DHC can be used to evaluate the scenarios that dominate D, which is the performance index associated with the slope seismic performance. This procedure is more consistent with performance-based engineering, compared to the procedure where only the IM deaggregation is used to identify the earthquake scenarios of most interest.

3.6. Uncertainty treatment using the polynomial chaos theory

When there is lack of robust alternative D models (e.g., subduction settings), the use of a logic tree scheme with few discrete branches may not be appropriate, because the epistemic uncertainty associated with the median D estimate cannot be captured. In these cases, the polynomial chaos theory (PC) can be used to quantify the epistemic

uncertainty. Macedo et al. (2020) present the formulation that uses the PC theory for the propagation of epistemic uncertainty in the median D for shallow crustal settings. Using the PC theory, a random process can be expressed as a linear combination of a family of orthogonal polynomials, where each polynomial is a function of random variables, and the coefficients in the expansion are deterministic. In our case, the random processes are associated with the median DHCs, where a particular D model is conceptualized as a sample from a continuous distribution of D models. If a normal distribution is considered for the epistemic uncertainty associated with the median D (visualized as hazard curves with normally distributed horizontal shifts for different hazard levels), then the different realizations for the epistemic uncertainty in the median D will derive in different hazard levels for a given d threshold, which will subsequently derive on a range of hazard curves. These hazard curves with normally distributed shifts can be represented as PC expansions. The mathematical details of the formulation are presented in Macedo et al. (2020) and Lacour and Abrahamson (2019); a brief summary is presented next. In the simplest form, a standard normal variable associated with different realizations of the median D can be defined as:

$$\eta = \frac{ln(\widehat{d}) - \mu_{EU}(IM, k_{yi}, T_{sj})}{\sigma_{EU}(IM, k_{yi}, T_{sj})} \tag{7}$$

where $ln(\widehat{d})$ is the median estimate from a D model and can be considered normally distributed (Macedo et al., 2018; Bray and Macedo, 2019; Rathje et al., 2014; Bray and Travasarou, 2007). The epistemic uncertainty in the median is considered normally distributed with a mean $\mu_{EU}(IM, k_{yi}, T_{sj})$ and a standard deviation $\sigma_{EU}(IM, k_{yi}, T_{sj})$. k_{yi} and T_{sj} represent realizations for the yield coefficient and fundamental period respectively, and are used to estimate μ_{EU} and σ_{EU} for a fixed *IM* level. Thus, the probability of exceeding a displacement threshold d (similar to Eq. (1)), considering a normal distribution for D can be expressed as:

$$P(D > d|IM,\ k_{yi},\ T_{sj},\ \eta) = 1 - \Phi\left(\frac{lnd - (\mu_{EU}(IMk_{yi}T_{sj}) + \eta \cdot \sigma_{EU}(IMk_{yi}T_{sj}))}{\sigma_{lnD}}\right) \tag{8}$$

The polynomial chaos theory can be used to discretize the uncertain conditional probability in Eq. (8). Hermite polynomials of the normal random variable η are used for the expansions because they guarantee optimal convergence for normally distributed variables. Thus, for a given displacement level d, Eq. (8) can be approximated by its polynomial chaos expansion as:

$$P(D > d\ IM,\ k_{yi},\ T_{sj}\eta) = \sum_{k=0}^{P} y_k(dIM)\Psi_k(\eta) \tag{9}$$

where $y_k(d, IM)$ are the deterministic coefficients in the expansion, P is the number of Hermite polynomials used in the expansion, and $\Psi_k(\eta)$ is the k-th Hermite polynomial evaluated at η. The results from the PC expansions in Eqs. (8) and (9) can then be combined with Eq. (1) to generate D hazard percentiles. The coefficients $y_k(d, IM)$ depend on the D threshold d and the *IM* level, and are provided in Macedo et al. (2020) for the case of shallow crustal settings.

In this study, we have developed GMMs that can be used in the context of PC expansions to generate IM realizations. The formulation of the PC-based GMMs are presented in Appendix A for both shallow crustal and subduction tectonic settings. This PC-based GMMs allow to automate the PC-based evaluations and are implemented in the computational platform discussed later. In addition, in this study, we have performed the PC-based implementation of the Bray et al. (2018) model for subduction settings, which was lacking in previous research efforts (the implementations in Macedo et al. (2020) are only for shallow crustal settings). The details of the implementation for the Bray et al. (2018) model in a PC-based framework are summarized in Appendix B. The Bray et al. (2018) D model considers a magnitude term in its functional form, therefore the PC coefficients $y_k(d, IM)$ are also magnitude-dependent (see Appendix B). In this case, DHCs should be computed as follows:

$$\lambda_D = \sum_{i=1}^{nky}\sum_{j=1}^{nTs}\int_{M_{min}}^{M_{max}}\int_0^{\infty} P(D > d \mid IM, M, k_{yi}, T_{sj}) f_M(M \mid IM)\Delta\lambda(IM)d(IM)d(M)w_i w_j \tag{10}$$

where $P(D > d|IM, M, k_{yi}, T_{sj})$ is the probability that D exceeds a given threshold d conditioned on *IM, M,* $k_{y,}$ and T_s, and $f_M(M|IM)$ is the conditional probability density function of the earthquake magnitude. The remaining terms were previously defined. All these procedures are available through the GUI platform developed in this study (details of the GUI are provided below).

4. Implementations

4.1. Graphical user interface platform

The new developments described in previous sections have been implemented in a MATLAB GUI, which allows a straightforward estimation of DHCs. The GUI allows accounting for the uncertainties associated with the different stages in the evaluation of DHCs (i.e., uncertainties associated with IMs, slope properties, and D models). The GUI has two main panels, the first panel (Fig. 3a) provides general information on the logic tree components specified by the user, and displays the resulting of DHCs after the calculations are completed (including the mean DHC estimate as well as percentiles or deaggregation of DHS by source and earthquake mechanism). The second panel (Fig. 3b), is used to define or edit the logic tree structure, including alternative IM hazard models, slope properties, and D models. In addition, this panel is used to define the inputs for PC-based estimations of DHCs. The platform can be accessed through GitHub at https://github.com/gacandia/SlopeDisplacements.

In addition to the estimation of DHCs (mean values, percentiles), which can be easily examined through graphical tools available in the GUI and exported for manipulation in other environments (e.g., Excel, text editors), the following novel features have been implemented in the GUI: deaggregation of the displacement hazard by source and earthquake mechanism, combination of hazard curves using weights assigned in a logic tree, automatic computation of DHC's percentiles, and parallelization in the computation of logic tree branches, which can significantly reduce runtimes.

4.2. Graphical user interface capabilities

4.2.1. Embedded seismic hazard toolbox

The GUI has embedded state-of-the-art deterministic and probabilistic seismic hazard capabilities to estimate the *IM* hazard and its variability, providing in this manner an automated logic to include the *IM* hazard in the evaluation of DHCs in the context of performance-based assessments. The seismic hazard capabilities embedded within the GUI are achieved through communication with the seismic hazard code developed by Candia et al. (2018, 2019). Through this integration, the GUI developed in this study allows the inclusion of custom (built in) or user-defined seismic source models, if required. In the current implementation, we offer seismic source models for Chile, Peru, Mexico, and Ecuador; in addition, the GUI can directly communicate with the USGS website for retrieving the IM hazard information in the United States. The GUI also allows the user to define information on seismicity parameters (e.g., activity rate in seismic sources), and multiple ground motion models. In this manner, if the information on seismic sources and seismicity parameters are available, the GUI can be used anywhere across the globe for the estimation of DHCs.

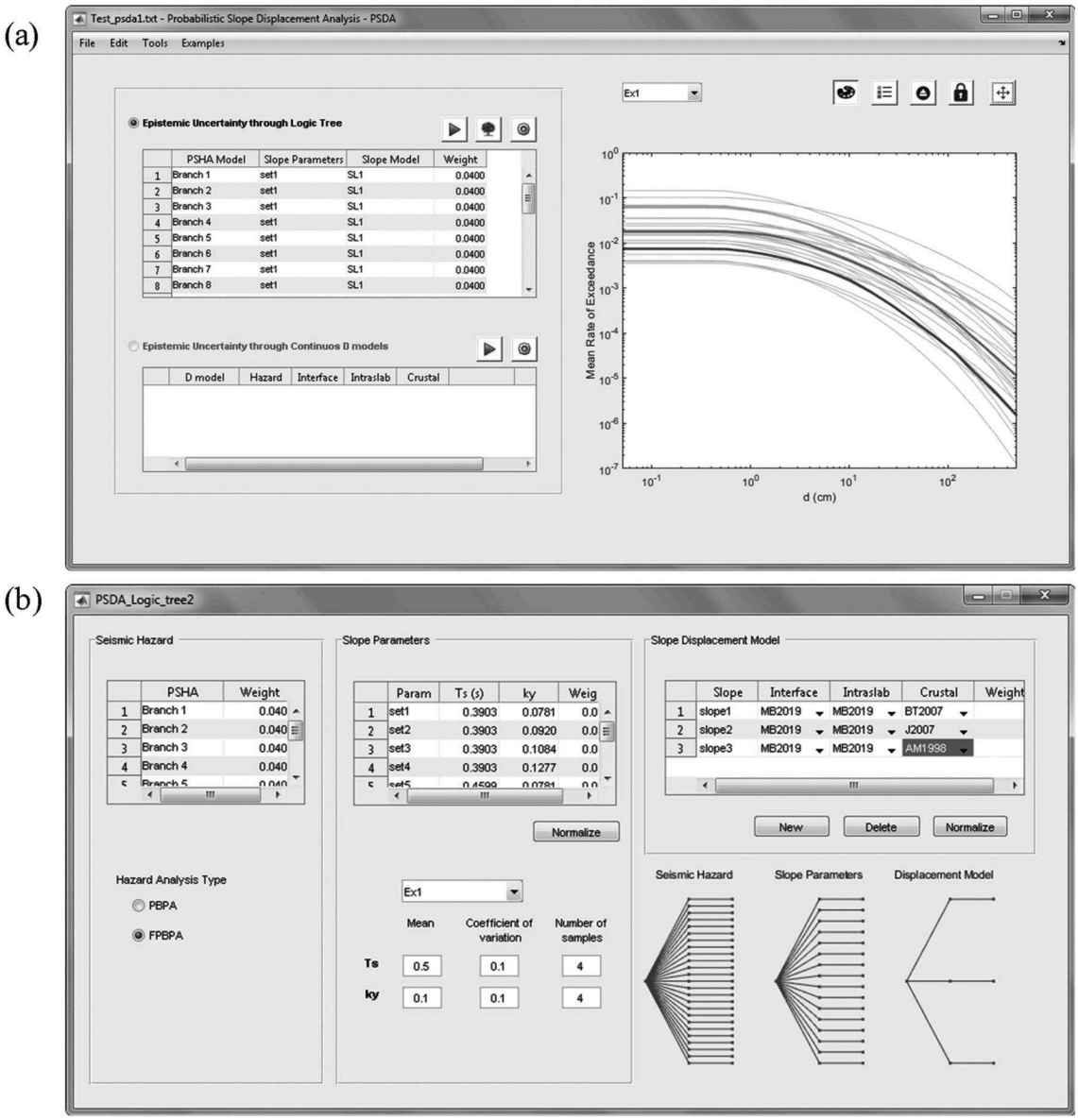

Fig. 3. Main panels in the developed MATLAB GUI to estimate DHCs: (a) panel to examine results; (b) D logic tree explorer.

4.2.2. Fully automated estimation of DHCs for D models with multiple IMs

When D models are formulated in terms of multiple IMs, a vector hazard evaluation (Bazzurro and Cornell 2002) is required to incorporate the joint hazard from different IMs into the estimation of DHCs. The implemented GUI has embedded vector hazard capabilities, which allow an automatic estimation of DHCs (e.g., see Fig. 4).

4.2.3. Evaluation of D hazard curves considering multiple tectonic settings

The implemented GUI features a library that includes a variety of D models, applicable to different tectonic settings. This allows a straightforward evaluation of DHCs for slope systems that are affected by earthquakes from multiple tectonic settings (i.e., shallow crustal, subduction), using the procedures previously discussed (Fig. 7 shows an example of this capability).

4.2.4. Uncertainty treatment in D hazard curves

The implemented GUI allows for a fully automated definition of logic trees to account for the epistemic uncertainty in the slope system properties as well as in alternative D models. In addition, it has fully automated PC-based capabilities that use the procedures previously described for uncertainty propagation.

5. Illustrative examples

In this section, we illustrate the application of the new developments and implementations previously presented in the context of engineering projects. All the calculations are performed within the GUI platform developed in this study.

The first example considers a shallow rigid slope system with $k_y = 0.2$ located on the Peruvian coast at coordinates S12.05° and W77.11°. In addition, we use the Saygili and Rathje (2008) D model, which is defined as:

$$\ln D = a_0 + a_1\left(\frac{k_y}{PGA}\right) + a_2\left(\frac{k_y}{PGA}\right)^2 + a_3\left(\frac{k_y}{PGA}\right)^3 + a_4\left(\frac{k_y}{PGA}\right)^4 + a_5 \ln PGA + a_6 \ln PGV \quad (11)$$

In Eq. (11), D is an explicit function of two IMs, i.e., PGA and PGV. Using the subduction sources for Peru defined by SENCICO (2016), the SIBER-RISK ground motion model for PGA and PGV (which is

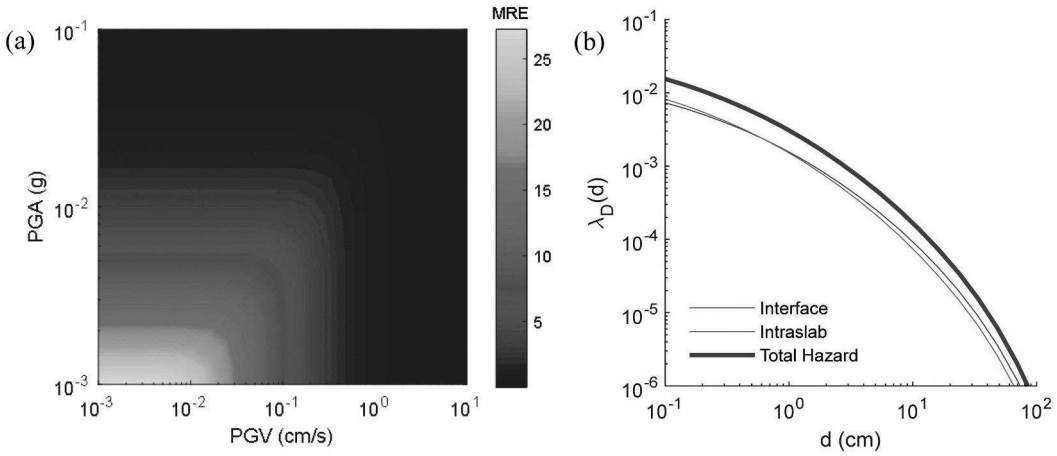

Fig. 4. Estimation of DHCs using a D model formulated in terms of two jointly occurring IMs. a) joint PGA(g) and PGV(cm/s) versus mean rate of exceedance (MRE) for a site in the Peruvian coast; and b) DHCs resulting from the convolution of vector hazard results with the Saygili and Rathje (2008) D model, considering a rigid slope with $k_y = 0.2$.

applicable to subduction zones), and a correlation coefficient of $\rho_{PGA,PGV} = 0.81$ (Candia et al. (2020), the resulting hazard estimation from a vector hazard analysis is shown in Fig. 4a. The vector hazard results are convolved with the Saygili and Rathje (2008) D model to produce the DHC shown in Fig. 4b. Notice that in this case, we used the Saygili and Rathje (2008) model just to show the coupling between vector hazard and the estimation of DHCs. Strictly speaking, a D model for subduction zones formulated in terms of 2 or more IMs should be used, but such a model is not available yet.

The second example consists of a 57 m high earth dam with a bedrock foundation (Fig. 5), the geometry and dynamic properties are identical to the example used by Bray and Travasarou (2007), who employed deterministic and pseudo-probabilistic procedures to assess D. The evaluation is performed for a deep slide through the dam, which is considered as the critical sliding surface (Bray and Travasarou, 2007). We will consider the PBPA and the FPPBA assessments to evaluate the seismic performance of the dam.

The best estimates for k_y and T_s are reported as 0.14 and 0.33 s, respectively. T_s is estimated using the measured shear wave velocities, considering a best estimate of Vs = 400 m/s. k_y is estimated using the results from pseudo-static slope stability analyses performed with the total stress strength properties of $c = 14\ kPa$ and $\phi = 21^\circ$ based on triaxial compression tests. Additionally, coefficient of variation values of 0.25 and 0.15 are considered for k_y and T_s respectively, which are in the medium range of the ranges provided by Macedo et al. (2018).

To illustrate the software capabilities handling multiple tectonic settings and the propagation of the ground motion uncertainty into the D-hazard, the system is hypothetically placed at two different locations, referred herein as Site 1 and Site 2. Site 1 is located in the Peruvian coast near Lima (S 11.18°; W 77.50°), and Site 2, is located in the Ucayali Department (S 10.084°; W 74.05°), 400 km northeast of Site 1; both sites have contributions from subduction (interface and intraslab) and shallow crustal earthquake zones. Fig. 6a shows the seismic sources defined by SENCICO (2016), an agency for seismic hazard assessment in Peru, along with the location of both sites. The selected D-models require scalar PSHA analyses for spectral accelerations, Arias Intensity, and vector hazard analyses for PGA and PGV, all of which are performed using the implemented GUI. In terms of spectral accelerations, we use the five GMMs from the NGA-West2 project (Bozorgnia et al., 2014) with equal weighs (i.e., 0.2) for the shallow crustal seismic sources. In the case of the subduction seismic sources, we use the Zhao et al. (2006), Montalva et al. (2017), and Abrahamson et al. (2016) with weighs of 0.25, 0.25 and 0.50 respectively. For PGV (shallow crustal sources only), we use the GMMs from the NGA-West2 project with equal weights (i.e., 0.2). Finally, for Arias Intensity, we use the conditional GMMs from Macedo et al. (2019), and Abrahamson et al. (2016), which are available in the implemented platform. The hazard curves for the spectral acceleration at the sliding mass degraded period (i.e., $T_d = 1.5T_s$) are shown in Figs. 6 b-e, the PGA hazard is shown in Fig. 6 c-f, and the results for the Arias Intensity hazard are shown in Fig. 6 d-g.

To incorporate the epistemic uncertainty associated with alternative D models, we use a logic tree approach, using the procedures described in the "new developments" section. The following models are considered for the shallow crustal zones: Jibson (2007), Rathje and Antonakos (2011), Bray and Travasarou (2007), and Bray and Macedo (2019), each model is assigned a weighting factor of 0.25. Even though the Jibson (2007) model should be strictly applicable to only rigid slopes, it was considered to illustrate the logic tree capabilities available in the platform when IMs such as AI are used. The results are not greatly influenced by this consideration. In the case of subduction

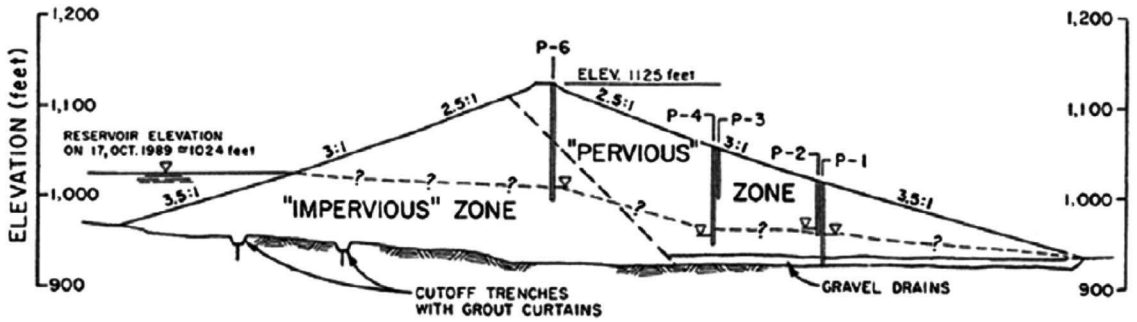

Fig. 5. Cross section of dam used in illustrative example (Adapted from Bray and Travasarou, 2007).

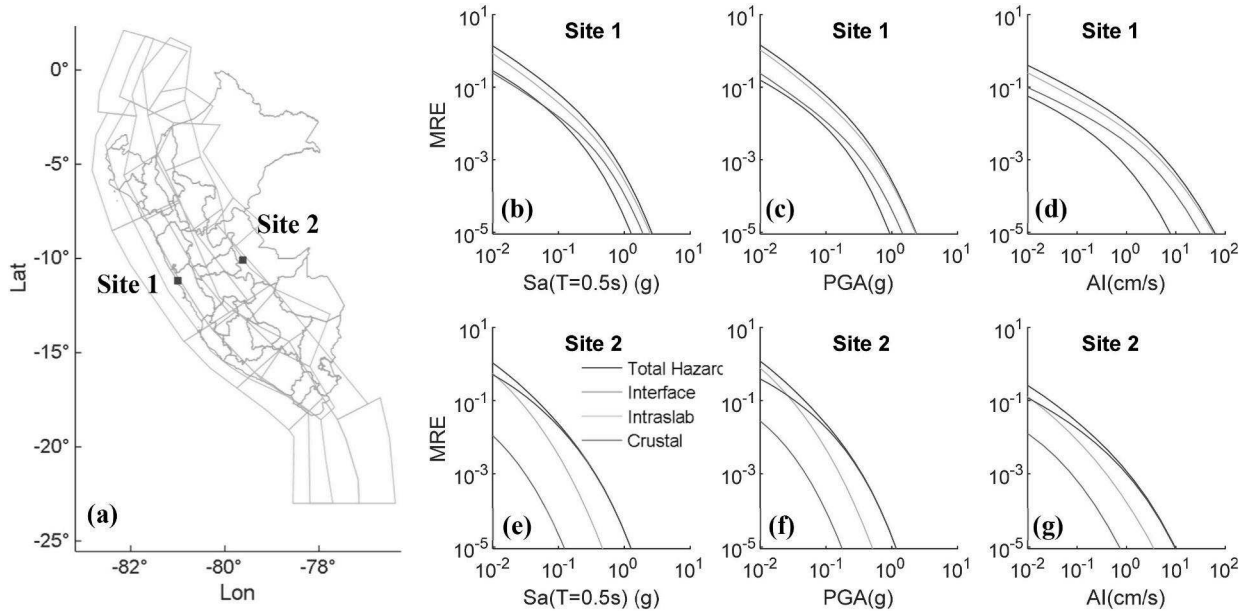

Fig. 6. Evaluation of the IM hazard for different IMs. (a) Seismic sources and evaluation sites (b,e) Hazard curves for the spectral acceleration at the sliding mass degraded period of 0.5 s. (c,d) PGA hazard results, and (d,g) Arias Intensity hazard curves. Fig. 6 (b-g) shows mean hazard curves for the A2016-ASK2014 branch disaggregated by earthquake mechanisms.

Table 1
Logic tree input used in the illustrative example.

Seismic hazard model			Slope parameters			Displacement models		
Subduction	Shallow crustal	w_k	Ts (s)	ky	w_t·w_j	Subduction	Shallow crustal	w_l
A2016	ASK2014	0.10	0.265	0.091	0.02	BMT2018	BT2007	0.25
M2017	ASK2014	0.05	0.265	0.141	0.10	BMT2018	RA2011	0.25
Z2006	ASK2014	0.05	0.265	0.217	0.02	BMT2018	JIB2007	0.25
A2016	BSSA2014	0.10	0.330	0.091	0.10	BMT2018	BM2019	0.25
M2017	BSSA2014	0.05	0.330	0.141	0.53			
Z2006	BSSA2014	0.05	0.330	0.217	0.10			
A2016	CB2014	0.10	0.411	0.091	0.02			
M2017	CB2014	0.05	0.411	0.141	0.10			
Z2006	CB2014	0.05	0.411	0.217	0.02			
A2016	CY2014	0.10						
M2017	CY2014	0.05						
Z2006	CY2014	0.05						
A2016	I2014	0.10						
M2017	I2014	0.05						
Z2006	I2014	0.05						

zones, we consider the Bray et al. (2018) D model, the only robust D model available to date for this tectonic setting. In the case of the Rathje and Antonakos (2011) model, alternative values for the mean ground motion period (T_m) are needed to account for its uncertainty; the selected values are 0.72 s, 1.00 s, and 1.39 s, with weights of 0.14, 0.72, and 0.14, respectively. This logic tree also considers three alternative values for T_s and three alternative values for k_y, with weights defined using a lognormal distribution based on the mean and covariance values for k_y and T_s. Table 1 summarizes the information used to define the logic tree, which combines nIM = 15 seismic hazard models, 9 pairs of slope parameters T_s and k_y, and 4 slope displacement models, resulting in 540 realizations of the epistemic uncertainty. In addition, the weight of a branch is computed as the product of the weights along the branch. This logic tree is easily defined in the implemented GUI using the inputs described above.

We first perform a PBPA assessment where only the mean IM hazard curve from the PSHA assessments is considered in the convolution with the D models. Fig. 7 shows the estimation of DHCs for Site 1, considering the contribution from shallow crustal and subduction tectonic settings. Fig. 7a displays the D hazard realizations as well as different percentiles. In addition, Fig. 7b shows the deaggregation of the DHC for the first logic tree branch in terms of the contribution from different tectonic settings. In this case, the subduction (interface and intraslab) seismic sources dominate the hazard associated with seismically induced slope displacements. Hence, they should be given higher weights on the selection of ground motions if more rigorous analyses are required (e.g., finite element analyses).

Next, we perform a FPPBA assessment (i.e., the full set of IM hazard percentiles are considered for each tectonic mechanism). The resulting DHCs for Site 1 and Site 2 are shown in Fig. 8a and b, respectively. Notice that the uncertainty about the mean D-hazard is significantly larger in Site 2, which is due to the higher variability of IM-hazard curves. Likewise, Fig. 8c and d show the D deaggregation corresponding to a 475 yrs. return period for Sites 1 and 2, respectively, considering the mean k_y and T_s values . From this analysis, it is apparent that the dominant scenario (deaggregation mode) for seismically-induced slope displacements at Site 1 is a subduction (interface or intraslab) event with magnitude 7.8 at a distance of 90 km, whereas, at Site 2, the

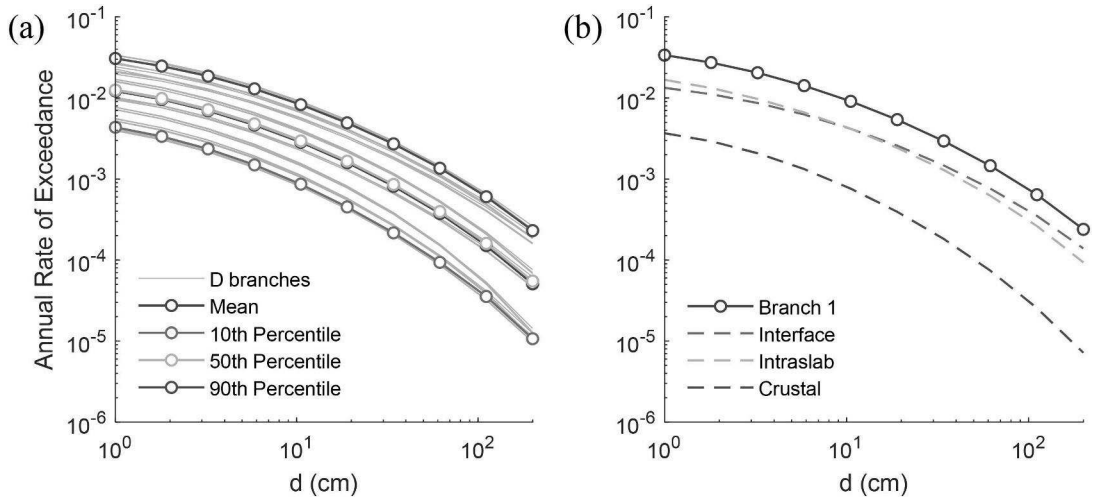

Fig. 7. Results of the PBPA assessment for Site 1 (a) total DHC shown mean and percentiles, (b) mean DHC from Branch 1 deaggregated by tectonic setting.

dominant scenario is a 6.8 magnitude shallow crustal earthquake at a distance of 50 km. This information would aid designers in the selection of ground motions to conduct rigorous numerical simulations of earth slopes if required (e.g., finite element analyses).

A direct comparison between the DHCs from the PBPA and FPPBA approaches is presented in Fig. 9. The median, as well as the 10th and 90th percentile estimates from both procedures, are similar at Site 1 due to the narrow range of the IM hazard curves at this location. On the other hand, the FPPBA approach yields a shifted mean D hazard curve and a broader range of D hazard percentiles at Site 2, which is influenced by the broader range of IM hazard curves at Site 2. These results suggest that the uncertainty of DHCs at Site 1 is dominated by the uncertainties of the slope system properties (i.e., k_y and T_s) and the alternative D models as opposed to the uncertainties in IM. On the other hand, the IM uncertainty dominates the DHC uncertainty at Site 2; and should be accounted for through a proper FPPBA assessment.

Finally, we illustrate the use of the PC theory to account for the epistemic uncertainty in the slope displacements using a realistic seismic source. In this example, we consider the slope system from the previous example (i.e., $k_y = 0.14$ and $T_s = 0.33s$, and coefficient of

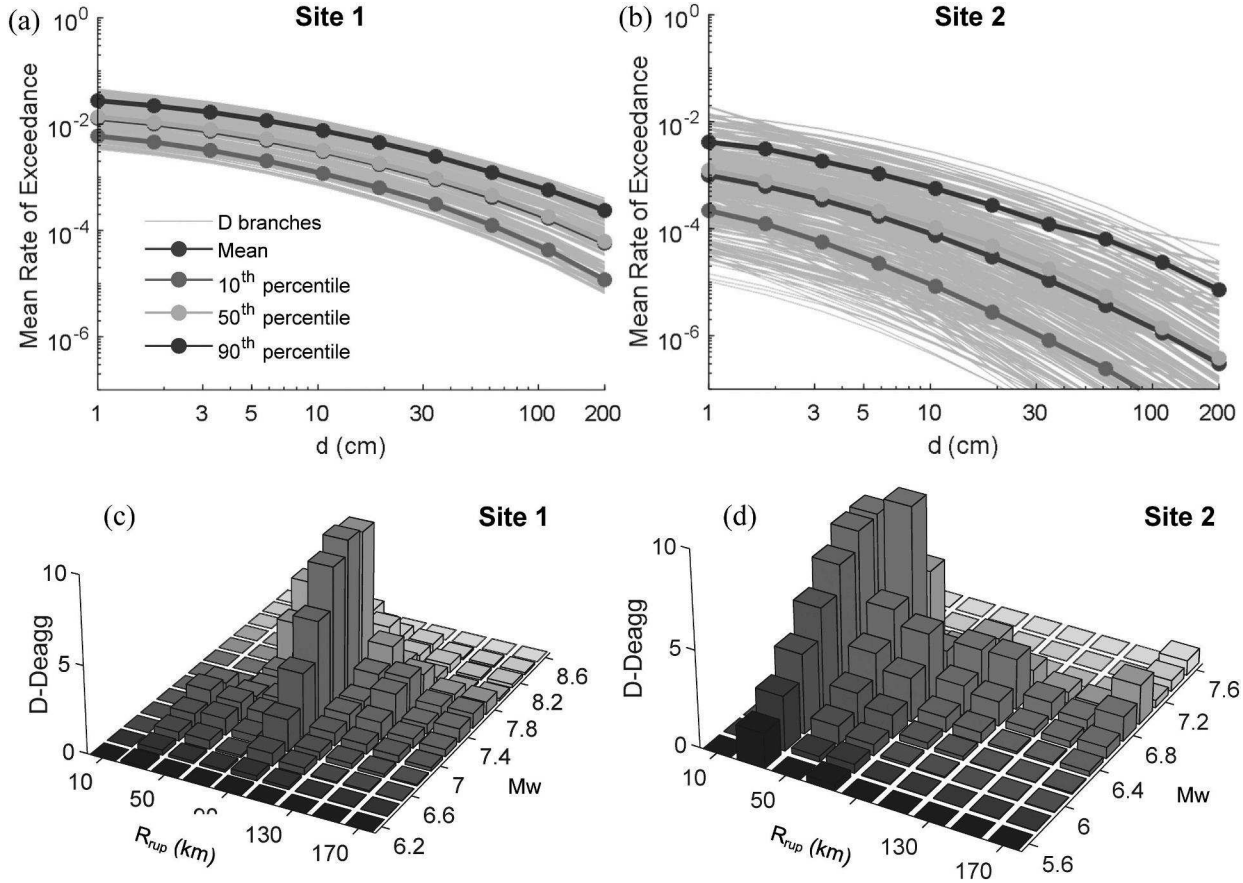

Fig. 8. Results of the FPPBA assessment showing 540 DHCs, mean and percentiles for (a) Site 1, and (b) Site 2; and D deaggregation for a 475 yrs. return period at (c) Site 1, and (d) Site 2.

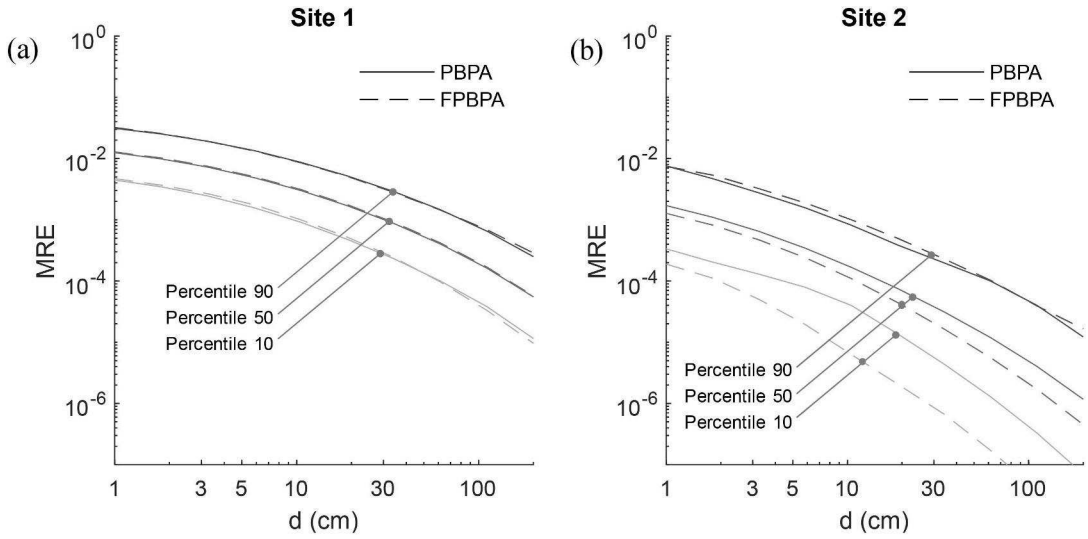

Fig. 9. Comparison of DHCs computed using the PBPA and FPBPA assessments for (a) Site 1 and (b) Site 2.

variation 0.25 and 0.15, respectively), located at Site 1 (S11.18°; W77.5°). For the sake of simplicity, we only include the seismic source F3 as defined by SENCICO (2016) for Peru, which is the closest subduction interface source to the evaluation point; the source boundaries and the evaluation point are shown in Fig. 10a. The calculation of the DHCs in this example uses the PC-based expansions of the Bray et al., 2018 model (formulated for subduction settings), which are described in Appendix B. In addition, we compare the PC-based approach with a standard logic tree calculation.

First, we evaluated the IM hazard and deaggregation and used these results as inputs for both the PC-based and logic tree approaches. In this manner, the comparisons between the two approaches are focused on the epistemic uncertainty treatment of D. The deaggregation and the IM hazard are presented in Fig. 10b, and Fig. 10c, respectively. The PC-based calculations were performed by generating 1000 realizations using lognormal distributions for k_y and T_s, with the properties previously described. In the case of the logic tree approach, the k_y and T_s discrete realizations were also generated using the same underlying distributions as in the PC-based aproach, considering 100 realizations. The DCHs calculated using the two approaches are presented in Fig. 10d. As it can be observed, the results from the PC-based and logic tree approaches are consistent in this case because the IM hazard inputs were the same, the underlying distributions for k_y and T_s were the same in the two approaches, and finally the same D model was employed. However, it is important to highlight that the PC-based approach is much faster, even with a much larger number of realizations (100 times faster in this case). The computational efficiency of the PC approach would be particularly important when a large number of analyses are needed as in regional-based simulations. Using the results from this example, and considering the 10th and 90th percentiles, the expected range of seismically-induced slope displacements are 2 cm to 10 cm, and 13 cm to 45 cm, for return periods of 475 and 2475 yrs, respectively. Similar comparisons could be performed in future studies considering different D models, when more models developed under consistent assumptions and data become available (see the discussion section).

6. Discussion

PBPA, FPPBA, or PC-based performance-based procedures should be preferred in engineering practice because they account for a more complete characterization of the uncertainties in the IM hazard and the properties of the sliding mass. Furthermore, these procedures produce D estimates that are consistent with design hazard levels (or return period), providing valuable input for a more rational, hazard-consistent, and risk-informed seismic design. The implementations provided by this study are intended to contribute to the application of performance-based procedures in engineering practice.

An important aspect to highlight for future studies is the need to develop more robust D models for both shallow crustal and subduction tectonic settings. Even in shallow crustal tectonic settings, where more D models exist, the few available models that can be applied to both rigid and flexible slopes have been developed using different databases and considerations. For example, the Bray and Macedo (2019) used 13422 ground motions from the NGA-West2 database and the spectral acceleration at $1.3T_s$. The Du et al. (2018) model used 3714 ground motions from the NGA-West2 database, and PGA combined with the spectral acceleration at 2.0 s as IMs. The Rathje and Antonakos (2011) model was based on a model for rigid slopes that used 2383 ground motions from the NGA-West1 database (Chiou et al., 2008), and it was adjusted based on 80 ground motions to constraint the expected seismic loading in flexible slopes using modified versions of *PGA* and *PGV*. This is in high contrast with the state of practice for IM models (e.g., the NGA-West2 for shallow crustal settings and the NGA-Sub project (Kishida et al., 2018) for subduction settings), which are developed under consistent databases and considerations. More D models will allow better treatment of epistemic uncertainties. In addition, since the PC-based approach considers a continuous distribution of D models, the development of more D models under consistent datasets and considerations will allow expanding the PC framework in future studies.

Finally, when more D models become available, future studies should explore their influence on the frameworks presented in this study, considering a large number of scenarios (i.e., areas with scarce, moderate, and active seismicity affecting a variety of slope systems). The developments in this study can be used in these future evaluations.

7. Conclusions

We have presented new developments and implementations for the seismic performance assessment of slope systems affected by earthquakes from multiple tectonic settings (i.e., shallow crustal and subduction earthquakes) under PBPA, FPPBA, and PC-based frameworks. These frameworks use the amount of seismically induced slope displacements and the associated hazard as indexes to evaluate the seismic performance of slope systems. All the new developments have been incorporated within a MATLAB-based graphical user interface (GUI), which is available at https://github.com/gacandia/SlopeDisplacements, to facilitate their use by engineers and

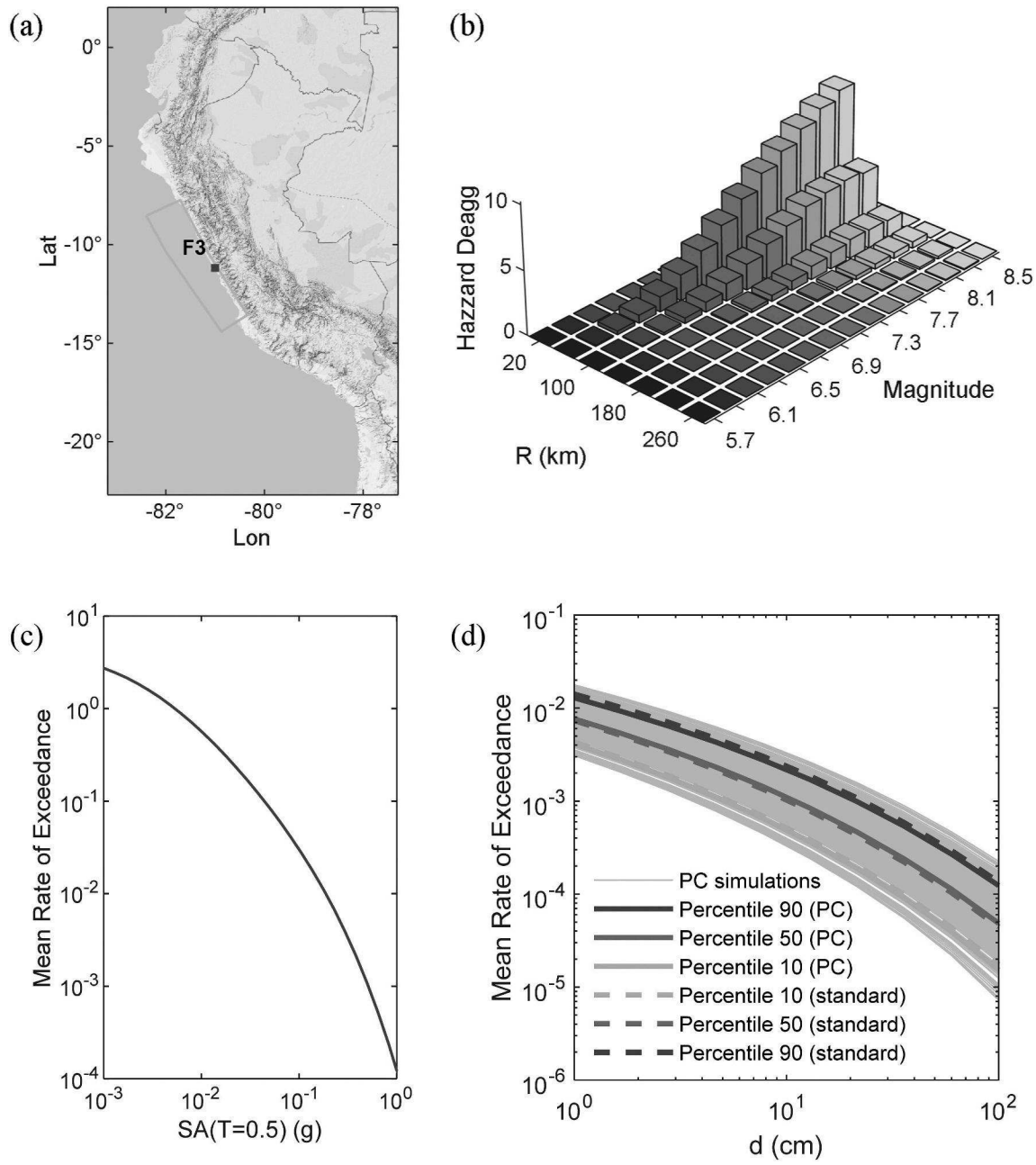

Fig. 10. Results of the assessment using the PC theory considering the seismic source F3 form SENCICO (a) seismic source and evaluation point, (b) 1000 PC simulations, 10th, 50th, and 90th percentiles computed from PC-based and the standard (logic tree based) estimation of D hazard curves.

researchers. Importantly, our implementations integrate the PSHA and DHCs evaluations, so they can readily be used in engineering practice with similar inputs as those required by a standard PSHA study.

In terms of the frameworks discussed in this paper, we recommend using FPPBA-based assessments for tectonic settings where logic trees for D models can be built (e.g., shallow crustal). This evaluation should be complemented by PBPA-based assessments to identify the drivers on the range of DHCs. As discussed in this study, if the uncertainty about the mean IM hazard curve is broad, it is expected that the IM hazard distribution will have a major influence in the range of D hazard percentiles. On the other hand, if the IM hazard curve percentiles cover a narrow range, it is expected that slope properties and the epistemic uncertainty on D models will dominate. In this case, results from PBPA and FPPBA approaches are expected to be similar. The main advantage of the PC-based approach is its computational efficiency, which would be particularly important when a large number of analyses are needed as in regional-based simulations. In addition, the PC-based approach allows the generation of continuous set of realizations for the median D that could represent a family of models. Under consistent inputs, PC-based and logic tree approaches would yield similar results, as illustrated in this study. Because of its computational efficiency, we recommend the use of the PC-based approach for subduction tectonic settings, where currently there is only one available robust D model. With more available D models in the future, more comparisons between PC-based and logic tree approaches should be performed as a subject of future studies.

Finally, we recommend using the DHC-based deaggregation procedure proposed in this study for identifying earthquake scenarios in the selection of ground motions when more rigorous evaluations (e.g., finite element analyses) of the seismic performance of a slope system are required. Importantly, the contribution of different tectonic settings to the seismic demand imposed on a slope system should be evaluated in

terms of the DCHs and not IM hazard curves. This contribution should dictate the selection of ground motions in a multiple tectonic setting environment (i.e., higher weights should be given to the tectonic setting that contributes the most to the D hazard).

Supplementary data to this article can be found online at https://doi.org/10.1016/j.enggeo.2020.105786.

Data availability

The platform developed in this article for the PBPA and FPPBA assessment of seismically induced slope displacements can be found at https://github.com/gacandia/SlopeDisplacements, as an open-source online data repository hosted at GitHub.

Declaration of Competing Interest

The authors declare that they have no known competing financial interests or personal relationships that could have appeared to influence the work reported in this paper.

Acknowledgments

This study has been possible thanks to financial support from the Georgia Institute of Technology through the start-up of Dr. Macedo. Also, Dr. Candia has received financial support from Facultad de Ingeniería Civil at Universidad del Desarrollo, the National Research Center for Integrated Natural Disaster Management ANID/FONDAP/15110017, and FONDECYT Grants N°11180937 “Seismic Risk of Mined Tunnels” and N°1170836 “SIBER-RISK: SImulation Based Earthquake Risk and Resilience of Interdependent Systems and Networks.” The authors are grateful for these supports.

References

Abrahamson, C., Shi, M., Yang, B., 2016. Ground-Motion Prediction Equations for Arias Intensity Consistent with the NGA-West2 Ground-Motion Models, PEER 2016/05 Report.

Bazzurro, P., Cornell, C.A., 2002. Vector-valued probabilistic seismic hazard analysis (VPSHA), Proc. of the 7th U.S. National Conf. on Earthquake Engineering. Earthquake Engineering Research Institute, Boston, Massachusetts 21-25 July 2002.

Bozorgnia, Y., Abrahamson, N.A., Atik, L.A., Ancheta, T.D., Atkinson, G.M., Baker, J.W., Baltay, A., Boore, D.M., Campbell, K.W., Chiou, B.S.-J., et al., 2014. NGA-West2 research project. Earthquake Spectra 30 (3), 973–987. https://doi.org/10.1193/072113EQS209M.

Bray, J.D., Rathje, E.M., 1998. Earthquake-induced displacements of solid-waste landfills. Geotech. Geoenviron. 124 (3), 242–253.

Bray, J., Macedo, J., 2019. Procedure for estimating shear-induced seismic slope displacement for Shallow Crustal Earthquakes. J. Geotech. Geoenviron. Eng. ASCE 142 (12), 04019106 (Accepted for publication).

Bray, J.D., Travasarou, T., 2007. Simplified procedure for estimating earthquake-induced deviatoric slope displacements. J. Geotech. Geoenviron. 133 (4), 381–392.

Bray, J.D., Macedo, J.L., Travasarou, T., 2018. Simplified procedure for estimating seismic slope deviatoric displacements in subduction zones. J. Geotech. Geoenviron. 3, 04017124. https://doi.org/10.1061/(ASCE)GT.1943-5606.0001833.

Candia, G., Macedo, J., Magna, C., 2018. An integrated platform for seismic hazard evaluation. In: 11th National Conference on Earthquake Engineering; Los Angeles, California.

Candia, G., Macedo, J., Jaimes, M.A., Magna-Verdugo, C., 2019. A New State-of-the-art platform for probabilistic and deterministic seismic hazard assessment. Seismol. Res. Lett. https://doi.org/10.1785/0220190025.

Candia, G., Poulos, A., de la Llera, J.C., Crempien, J.G., Macedo, J., 2020. Correlations of spectral accelerations in the Chilean subduction zone. Earthquake Spectra 36 (2), 788–805.

Chiou, B., Darragh, R., Gregor, N., Silva, W., 2008. NGA project strong-motion database. Earthquake Spectra 24 (1), 23–44.

Du, W., Wang, G., Huang, D., 2018. Evaluation of seismic slope displacements based on fully coupled sliding mass analysis and NGA-West2 database. J. Geotech. Geoenviron. Eng. 144 (8), 06018006. https://doi.org/10.1061/(ASCE)GT.1943-5606.0001923.

Jibson, R.W., 2007. Regression models for estimating coseismic landslide displacement. Eng. Geol. 91 (2–4), 209–218.

Kishida, T., Contreras, V., Bozorgnia, Y., Abrahamson, N.A., Ahdi, S.K., Ancheta, T.D., Boore, D.M., Campbell, K.W., Chiou, B., Darragh, R., et al., 2018. NGA-Sub ground-motion database. In: Proc. 11th National Conference on Earthquake Engineering, Los Angeles, California, 25–29 June.

Lacour, M., Abrahamson, N.A., 2019. Efficient propagation of epistemic uncertainty in the median ground-motion model in probabilistic hazard calculations. Bull. Seismol. Soc. Am. https://doi.org/10.1785/0120180327.

Lin, J.-S., Whitman, R.V., 1986. Earthquake induced displacements of sliding blocks. J. Geotech. Eng. 112 1 (44), 44–59. https://doi.org/10.1061/(ASCE)0733-9410.

Macedo, J., 2017. Simplified procedures for estimating earthquake-induced displacements. Ph.D. thesis. Dept. of Civil and Env. Eng., Univ. of California, Berkeley.

Macedo, J., Bray, J., Travasarou, T., 2017. Simplified procedure for estimating seismic slope displacements in subduction zones. In: 16th World Conference on Earthquake, 16WCEE 2017; Santiago, Chile.

Macedo, J., Bray, J., Abrahamson, N., Travasarou, T., 2018. Performance-based probabilistic seismic slope displacement procedure. Earthquake Spectra 35 (2), 673–695.

Macedo, J., Abrahamson, N., Bray, J.D., 2019. Arias Intensity Conditional Scaling Ground-Motion Models for Subduction ZonesArias Intensity Conditional Scaling Ground-Motion Models for Subduction Zones. Bull. Seismol. Soc. Am. 109 (4), 1343–1357.

Macedo, J., Lacour, M., Abrahamson, N., 2020. Epistemic uncertainty treatment in seismically-induced slope displacements using polynomial Chaos. J. Geotech. Geoenviron. Eng. ASCE. https://doi.org/10.1061/(ASCE)GT.1943-5606.0002345. (Accepted for publication).

Makdisi, F., Seed, H.B., 1978. Simplified procedure for estimating dam and embankment earthquake-induced deformations. J. Geotech. Eng. 104 (7), 849–867.

Montalva, G., Bastias, N., Rodriguez-Marek, A., 2017. Ground motion prediction equation for the Chilean subduction zone. Bull. Seismol. Soc. Am. 107, 2. https://doi.org/10.1785/0120160221.

Newmark, N., 1965. Effects of earthquakes on dams and embankments. Geotechnique. 15 (2), 139–160.

Rathje, E.M., Antonakos, G., 2011. A unified model for predicting earthquake-induced sliding displacements of rigid and flexible slopes. Eng. Geol. 122 (1), 51–60.

Rathje, E.M., Saygili, G., 2011. Pseudo-probabilistic versus fully probabilistic estimates of sliding displacements of slopes. J. Geotech. Geoenviron. Eng. ASCE 137 (3), 208–217.

Rathje, E.M., Wang, Y., Stafford, P.J., Antonakos, G., Saygili, G., 2014. Probabilistic assessment of the seismic performance of earth slopes. Bull. Earthq. Eng. 12 (3), 1071–1090.

Richards, R., Elms, D.G., 1979. Seismic behaviour of gravity retaining walls. J. Geotech. Eng. Divi. ASCE 105 (4), 449–464.

Saygili, G., Rathje, E.M., 2008. Empirical predictive models for earthquake-induced sliding displacements of slopes. J. Geotech. Geoenviron. Eng. ASCE 134 (6), 790–803.

Saygili, G., Rathje, E.M., Wang, Y., El-Kishky, M., 2018. Cloud-based tools for the probabilistic assessment of the seismic performance of slopes. In: Geotechnical Earthquake Engineering and Soil Dynamics V, https://doi.org/10.1061/9780784481486.003.

Sencico, 2016. Actualización del programa de cómputo orientado a la determinación del Peligro Sísmico en el país. Servicio Nacional de Capacitación para la Industria de la Construcción. Lima, Peru. In Spanish.

USGS, U., 2017. Unified Hazard Tool. U.S. Geological Survey. URL. earthquake.usgs.gov/hazards/interactive.

Wang, Y., Rathje, E., 2015. Probabilistic seismic landslide hazard maps including epistemic uncertainty. Eng. Geol. 196, 313–324.

Watson-Lamprey, J., Abrahamson, N., 2006. Selection of ground motion time series and limits on scaling. Soil Dyn. Earthq. Eng. 26 (5), 477–482.

Zhao, J.X., Zhang, J., Asano, A., Ohno, Y., Oouchi, T., Takahashi, T., Ogawa, H., Irikura, K., Thio, H.H., Somerville, P., Fukushima, Y., 2006. Attenuation relations of strong ground motion in Japan using site classification based on predominant period. Bull. Seismol. Soc. Am. 96 (3), 898–913.